

CHARACTERIZATION OF ACOUSTIC SOFTENING OF ALUMINUM 6061 WITHIN A PLASTICITY FRAMEWORK

Q. Mao, N. Coutris, and G. Fadel
Department of Mechanical Engineering, Clemson University, SC 29630

REVIEWED

Abstract

Ultrasonic additive manufacturing (UAM) is a rapid prototyping technology that features a metal joining process through ultrasonic welding. The bonding mechanisms and mechanics of UAM have been investigated for decades. Meanwhile, the plastic deformations of metals were extensively studied by many researchers for their significant roles in bond formation. However, most of these research efforts considered solely the surface frictional effects on plastic deformation whereas the volumetric effects of ultrasound were rarely considered. This paper investigates the effects of ultrasound on deformation of Aluminum 6061 through experimental studies and highlights the volumetric effects of ultrasound, i.e. the “acoustic softening”: a stress reduction on the stress-strain relation of Aluminum 6061 upon application of ultrasounds. Based on observations obtained from a designed experimental setup, a phenomenological model is proposed to characterize the acoustic softening effects in terms of the ultrasonic intensities. Additionally, by modifying Hockett’s plasticity model, a plasticity frame work is established to characterize the deformation of Aluminum 6061 in UAM. The acoustic softening model is then incorporated into the plasticity framework. The complete model is then validated by comparing its predictions with experimental measurements.

1. Introduction

The ultrasonic additive manufacturing (UAM) is a solid state fabrication process that combines an additive process of joining metal foils through ultrasonic metal welding and a subtractive process of CNC contour milling. The additive process bonds thin metal foils of 100 – 150 μm thickness to the substrate layer by layer with combined application of ultrasonic energy and compression, whereas the subtractive process shapes the deposited layers to the required contour with CNC milling. The bonding mechanism of UAM has been studied for decades yet no uniform conclusion has been achieved. Metallurgical adhesion is supported by many researchers [1-7] as the bonding mechanism during which material plastic deformation plays a vital role in closing and filling voids at the contact interface. Diffusion across the weld interface is supported by some investigations based on the observation of high plastic strain rate during the ultrasonic welding near the bonding interface, which significantly enhances diffusion by increasing vacancy concentrations within materials [8, 9, 10]. Similar observations are made by other researchers, who claim that the high vacancy concentration caused by the high strain rate significantly depresses material melting temperature, thus allowing localized melting to occur [10]. Recrystallization is also proposed as a cause of bonding [5, 10, 11]. It is believed that plastic deformation and temperature rise due to the continuous input of ultrasonic energy provide the necessary driving force for recrystallization. Mechanical interlocking is reported by a few researchers [7] who studied the bonding of dissimilar materials in a combination of one material

being soft and the other hard. Severe plastic deformation is observed in the soft material. Despite the divergence among the competing theories, all the investigations show the significance of plastic deformation of materials in promoting bonds formation regardless of its causes. It is widely accepted that plastic deformation promotes bonds formation by dispersing surface oxides and contaminants, increasing contact areas of pure metal, and maintaining the already formed bonds [2, 5]. As a result, the material plasticity in UAM requires a comprehensive investigation and characterization to fully understand the bonding process.

Ultrasonic energy, being the major energy input of UAM, affects material plasticity in terms of surface and volumetric effects. The surface effect includes friction-induced plastic deformation at the mating surface and frictional heating that reduces the plastic yield stress of materials by increasing temperature, i.e. the “thermal softening”. The volumetric effect refers to a unique effect of ultrasound on the volume of metals: the stress required for plastic deformation is reduced upon application of ultrasound, known as the “acoustic softening”. This effect is believed to affect the plasticity of metals more effectively than thermal softening with less energy input [2, 5, 12-14]. While the surface effects of ultrasound have been extensively studied, the volumetric effects are considered by only a few researchers in studies of UAM [13, 14]. This paper investigates the acoustic softening of aluminum 6061 which is a material extensively used in UAM, and characterizes the acoustic softening using a selected plasticity model, aiming at establishing an analytical material plasticity framework for future studies of UAM.

Despite the limited investigations on volumetric effects of UAM, the physics of acoustic softening in metals have been under investigation since the 1950s [15]. The acoustic softening is first documented by Blaha and Langenecker, who applied tensile tests with superposition of ultrasound on a variety of metals: aluminum single crystals and polycrystals, coppers, nickels, magnesium and titanium [12, 16]. According to these researchers, the acoustic softening takes place instantaneously as ultrasound starts and the tensile stress drops abruptly. The stress returns to its original value as soon as the ultrasound is switched off. The stress reduction is observed to be “proportional” to the ultrasound intensity [12]. However, when the ultrasonic intensity exceeds a certain threshold, a “residual hardening” is observed, i.e., the stress returns to a value higher than its original value as the ultrasound is switched off. Additionally, based on the stress-strain examination, the curve is observed to be similar to thermal softening, yet the consumption of ultrasonic energy is of the order of 10^6 less than thermal energy for the same amount of stress reduction. Later, many researchers investigated the acoustic softening. Some conducted experiments similar to Langenecker’s but reported different observations [17-20]. For instance, Nevill and Brontzen [17] claimed that stress reduction is a linear function of vibration amplitude rather than being proportional to ultrasonic energy. Others designed different experimental setups and obtained conflicting observations [21, 22]. For instance, Culp conducted compression tests on aluminum alloy 6063 with superposition of ultrasound and reported “residual softening” instead of “residual hardening” [21]. Yao et al. performed compression tests superimposed with sound waves of 9.8 kHz which is below the frequency range of ultrasound and reported residual hardening when the sound wave stopped [22]. The divergences among experimental observations in the literature renders the modeling of acoustic softening challenging and thus experiments on acoustic softening are necessary and crucial in quantifying the stress reduction in terms of ultrasonic energy levels.

In a tensile/compression test, acoustic softening couples with strain hardening in the plastic deformation region. Consequently, the acoustic softening model has to be incorporated into a plasticity model that accounts for strain hardening. Kelly et al. introduced acoustic softening into a power law model proposed by Hockett which characterizes strain hardening and thermal softening [14]. The power law equations are derived from true stress versus true strain relations of aluminum 1100-O in the plastic deformation region over a range of strain rates and temperatures by varying the coefficient and the exponent [24]. By assuming that acoustic softening linearly affects the true stress, Kelly et al. modified the plasticity model and introduced acoustic softening factor [14]. Though the modified model gives a prediction that resembles the experimental observations by Blaha and Langenecker, the assumption of acoustic softening linearly affecting stress lacks experimental support. Additionally, the material used in Langenecker's experiment is aluminum single crystals whereas the material being characterized by Kelly et al. is commercially pure aluminum 1100-O, which has a polycrystalline structure. Siddiq et al. established a thermal-mechanical material model of UAM which is solved using finite element methods [25]. The model characterizes plasticity of aluminum 6061 under cyclic loading. It combines a nonlinear isotropic model and a kinematic hardening model which are proposed by Chaboche and his coworker [26]. The model is readily available in ABAQUS and is subject to modification. The acoustic softening is introduced by modifying the isotropic and kinematic hardening rules. The assumption made about acoustic softening is that the stress reduction is proportional to ultrasonic intensity, which is reported by Blaha and Langenecker, and Green. [16, 27]. However, the model is subject to debate since Siddiq et al. model for aluminum 6061 using experimental data of aluminum single crystals [25]. By comparing the experiment data and those reported by Blaha and Langenecker, this paper demonstrates that the stress reduction in polycrystalline aluminum alloy is significantly different from that in aluminum single crystals. Other models that have been applied to UAM include crystal plasticity models [22, 28]. By using the Crystal Plasticity Finite Element Method (CP-FEM) which is readily available in ABAQUS, a cube of polycrystalline material is constructed using the electron backscattered diffraction (EBSD) data of aluminum alloy 6061[28]. The acoustic softening is introduced by modifying the plastic flow rule and by adding an ultrasonic softening term which is a function of ultrasound intensity. The assumption about the softening term comes from the observation by Blaha and Langenecker that the decrease in yield limit is directly proportional to the ultrasound energy input. However, the softening term is derived as a polynomial of ultrasound intensity. The softening term is not proportional to ultrasound intensity and it is difficult to determine the order of the polynomial without experimental data. Yao et al. utilized the thermal activation model proposed by Kocks and the dislocation evolution law proposed by Krausz and Krausz to account for acoustic softening and residual hardening within a crystal plasticity frame work [22, 29, 30]. The underlying assumptions are that the dislocations overcome obstacles with the assistance of thermal energy as ultrasound starts and that the dislocations evolve and tangle with each other to cause residual hardening as ultrasound stops [22]. The acoustic softening model relies heavily on the assumed mechanism of thermal activation at dislocations whereas the actual mechanisms of acoustic softening remain subjective to debate.

In summary, it is shown that the bonding process of UAM is significantly influenced by plasticity of the materials in use and that the material plasticity is influenced by surface and volumetric effects of ultrasound. However, the effect of ultrasound on UAM, specifically the

volumetric effect has not been fully investigated and characterized. The existing literature reports diverging observations of acoustic softening on different metallic materials, making it difficult to characterize for a specific metal without conducting experiments. Most of the existing analytical models of acoustic softening reviewed lack support of experimental data. To the best knowledge of the authors, no experimental investigations have been reported regarding acoustic softening of aluminum 6061. In this paper, an experimental setup similar to Langenecker's is used to observe acoustic softening on aluminum 6061. Stress reductions in plastic region are measured and stress strain curves are recorded at different levels of ultrasound intensities. Based on the experimental observations, an analytical phenomenological model is proposed to characterize the acoustic softening in the plastic region combined with strain hardening effect. By comparing the predictions from the analytical model and the experimental data, it is shown that the proposed model is able to characterize the acoustic softening effect with good accuracy.

2. Experimental Setup

Fig.1 shows the scheme of the experimentation which is similar to Langenecker's testing apparatus. It consists of an MTS hydraulic tensile test machine, a Branson 2000 ultrasonic plastic welder and a rigid frame made of aluminum 6061. The MTS tensile test machine applies tensile or compression force in the vertical direction to the bottom end of the specimen while the ultrasonic plastic welder provides longitudinal ultrasonic vibration to the top of the specimen. A load cell that connects the MTS actuator and the specimen is used to record the loading profile. The ultrasonic plastic welder consists of an ultrasonic transducer that converts electric energy into ultrasonic vibration with a fixed frequency of 20 kHz, a booster that amplifies vibration and an ultrasonic horn that further amplifies vibration and delivers ultrasonic energy to the specimen. A circular high gain horn made of aluminum heat-treated alloy is used and the maximum vibration amplitude is 48 microns. Due to the fact that the ultrasonic welder is designed to take compressional load rather than tensile load, the ultrasonic horn cannot be connected to the specimen that is tensioned by the MTS machine. As a result, a box frame made of aluminum 6061 plates with thickness of 0.5 inches is designed to provide a mounting position for the specimen and to take the tensile load off the ultrasonic welder. The specimen is installed such that it is oscillated by the ultrasonic horn at the top end, fixed at a point right below the oscillating point and is tensioned at the bottom end. The specimen is in cylindrical shape with two fillets to transit from large installation diameter to small testing diameter without causing undesired flexure in the machining process (fig.2). In the gage section, the diameter is 3/16 inch and the length is 1 inch. The specimen is made of aluminum 6061 for its extensive application in UAM. Apart from the testing system, a Polytec laser vibrometer is used to measure the maximum vibration amplitude available in the test. In addition, A FLIR thermal camera and Omega DP490 thermal couples are used to observe the temperature of the specimen surface close to the deformation region. Different experimental setups have been proposed with variation in tensile or compression tests, and in longitudinal or transversal vibration [12, 22, 27, 31-34]. Among the various setups, the combination of tensile test and longitudinal ultrasonic vibration proves to be most effective in reducing friction-induced heating which potentially introduces thermal softening as noise to acoustic softening [23]. The setup is therefore adopted in this paper.

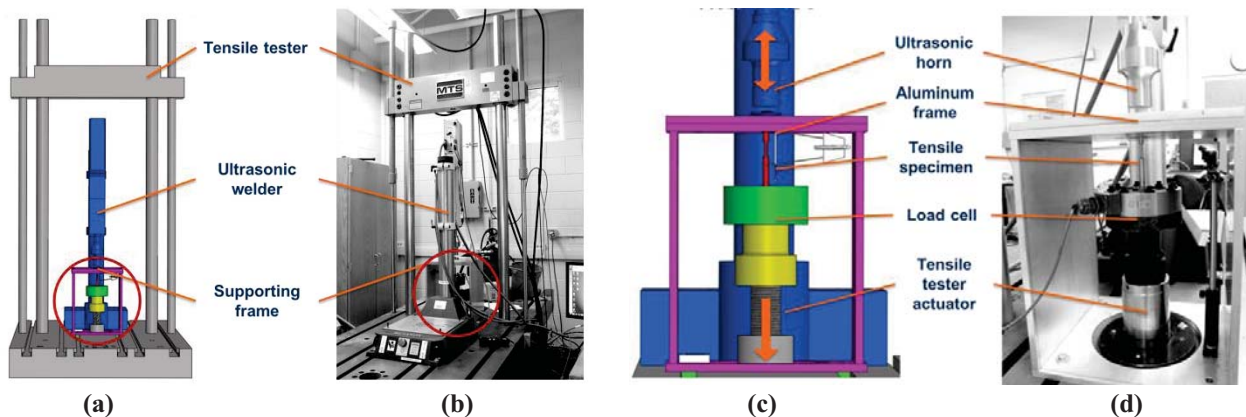


Fig. 1 Experimental setup: (a) CAD model, (b) the actual setup; frame Design: (c) the CAD model, (d) the actual frame

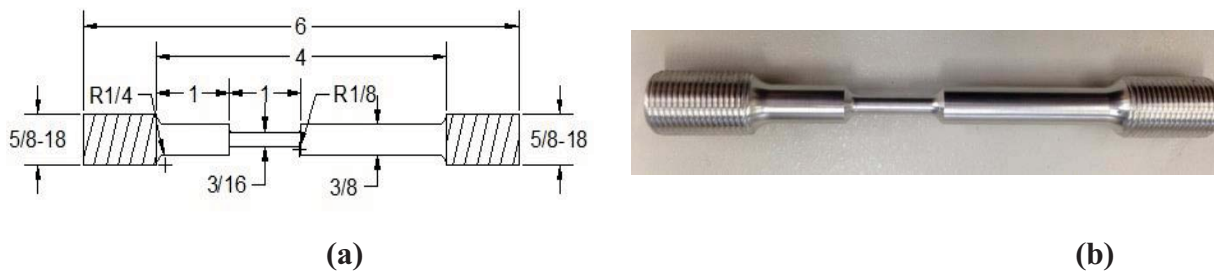


Fig. 2 Specimen design (a) specimen dimensions (unit: inch), (b) the actual specimen

3. Experimentation Details and Observations

In order to characterize the acoustic softening in the plastic deformation region under different levels of ultrasonic energy in aluminum 6061, a series of tensile tests are run as the input of ultrasonic energy varies. The specimen is subjected to static tensile load at a constant loading speed of 0.1 mm/s until it fails. Meanwhile, the ultrasonic welder is started when the specimen begins to yield. As the welder starts, the ultrasonic horn is brought into contact with the upper end of the specimen at a constant speed and is compressed on top of the specimen with a moderate force of around 100 lbs. Then the ultrasound starts and the longitudinal ultrasonic wave propagates through the specimen that is being tensioned. The ultrasonic irradiation lasts for 10 seconds before it stops. The compression is then removed and the ultrasonic horn is brought up. The amount of ultrasonic energy applied during the irradiation is recorded by the welder controller and can be retrieved when the test completes. Among the 26 tests that are completed with success, 6 tests are selected to present their stress strain curves at different levels of ultrasonic energy input: 0 J, 915J, 2684 J, 3718 J, 5506 J and 6040 J. By setting the maximum ultrasonic energy input as the 100% energy level, the energy inputs are converted into percentages for clarity. Fig. 3 shows the engineering stress strain curves of aluminum 6061 at 6 different levels of energy input. As the ultrasonic energy level increases, the stress reduction increases accordingly and the material becomes “softer”. In the four lowest energy levels, the softening curves show a combined effect of acoustic softening, i.e. stress reduction, and strain hardening. In the other two high energy levels however, the strain hardening diminishes and the

curves become straight lines, which are similar to curves reported by Blaha and Langenecker when ultrasonic intensity is large [12]. During the experiment, a thermal camera is used to record the temperature gradient at the acoustic softening spot. Two thermal couples are glued to the surface of the spot to identify the temperature increase. The room temperature is 70 °F and the highest temperature observed during ultrasonic irradiation is 120°F. Due to the high temperature (400 °F) required for thermal softening to show significance [16], the thermal softening in our experiment is considered as insignificant.

Fig.4 shows the comparison of our experimental data with that of Blaha and Langenecker. The engineering stresses and strains measured from experiments are first converted into true stresses and strains. The true strain is then converted to plastic strain using the equation:

$$\epsilon_p = \epsilon_{tr} - \frac{\sigma_{tr}}{E} \quad (1)$$

where ϵ_p is plastic strain, ϵ_{tr} is true strain, σ_{tr} is true stress and E is the Young's modulus. From the comparison, several observations can be made: 1) the yield strength of aluminum 6061 which is used in our experiment is much higher than the yield strength of aluminum single crystals used in Blaha and Langenecker's experiments. The yield strength of aluminum 6061 is 37.2 kg/cm² whereas the yield strength of aluminum single crystals is around 1.5 kg/cm². 2) The ultrasound intensities used in our experiment are two orders of magnitude higher than the ultrasound intensity used in Langenecker's experiment [12], yet the stress reductions achieved in our experiment are much lower. 3) Instead of residual hardening, moderate residual softening is observed in stress strain relations as soon as the ultrasound stops. The residual softening then dies down as plastic deformation continues, possibly due to the dissipation of previously stored acoustic energy [21]. These observations demonstrate that the acoustic softening in aluminum alloys is quantitatively different from the acoustic softening in aluminum single crystals. It takes much higher ultrasonic energy to achieve the same stress reduction in aluminum 6061 than in aluminum single crystals. Therefore the material characterization has to be derived from the experimental data of the same material.

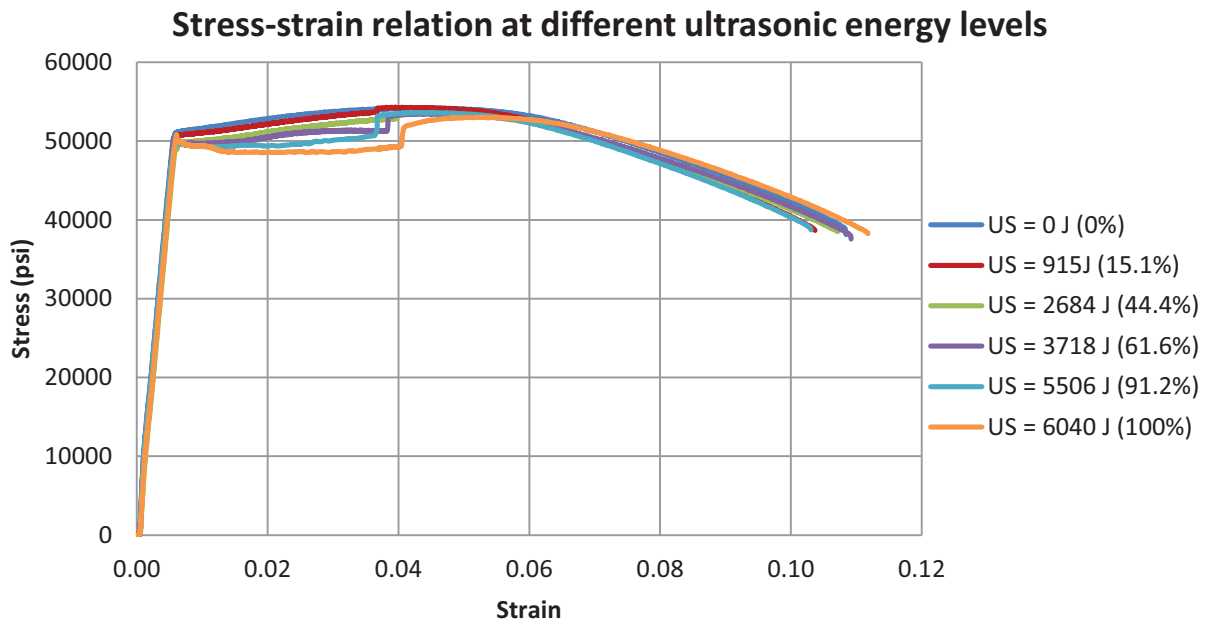


Fig.3 The engineering stress-strain relations at different levels of ultrasound (US).

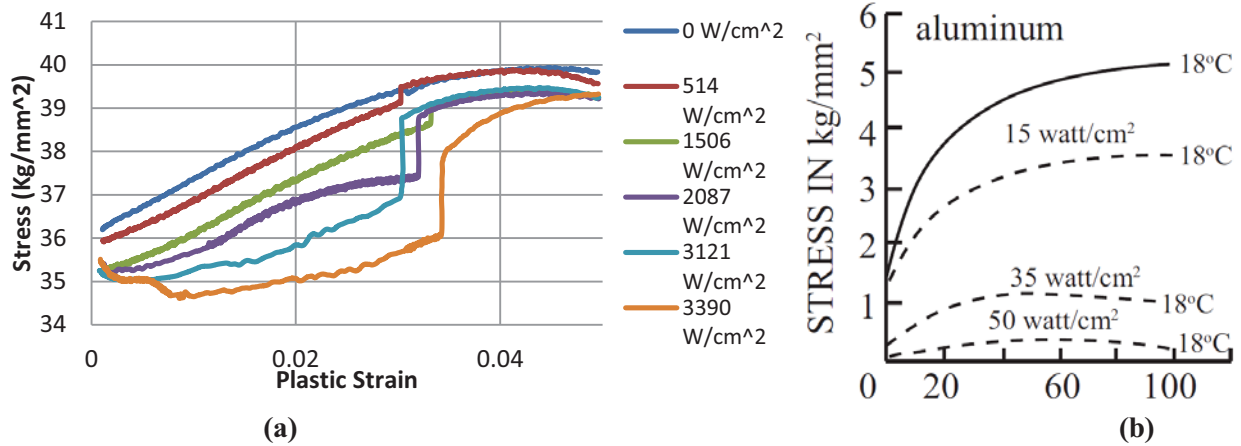


Fig.4 The comparison of stress-strain relations with that of Blaha and Langenecker. (a) Our experimental data (b) Langenecker's experimental data

4. Analytical Model

With the acoustic softening effect observed and experimental data collected, a phenomenological model is required to incorporate acoustic softening effect into the stress strain relations of the material used for studies of UAM. The stress strain curves present deformation in elastic and plastic regions. In the elastic deformation region, no ultrasound is applied in this experiment since elastic deformation is not the focus of this paper. According to previous studies [23] however, the application of ultrasound does not change the Young's modulus of material. Therefore the value of the Young's modulus is calculated from the true stress strain data $E = 95646$ ksi. In the plastic deformation region, acoustic softening is observed to be coupled with strain hardening. As a result, the analytical model has to incorporate an equation that characterizes the hardening in the stress and strain relation. Hockett utilized power law equations to characterize the relation between stress and strain as strain rate and temperature change [24]. The equation is shown to be able to effectively capture the hardening curve measured in experiments. Therefore we introduce the power law equation to account for the hardening effect in our experiment:

$$\sigma_t = K \varepsilon_t^n \quad (2)$$

Where σ_t the instantaneous true stress is required for plastic deformation, ε_t is true strain, K is the strength coefficient and n is the strain hardening coefficient. K and n are constants determined by fitting the power law equation to the stress-strain data free of ultrasonic irradiation. Therefore the engineering stress-strain data are first converted to true stress versus true strain data using the relation:

$$\varepsilon_t = \ln(1 + \varepsilon_e) \quad (3)$$

$$\sigma_t = \sigma_e (1 + \varepsilon_e) \quad (4)$$

where ε_e is engineering strain and σ_e is engineering stress. Since the above conversion applies only to plastic deformation without necking, the curves are truncated at the point when necking occurs. The true stress versus true strain curves are shown in fig.5. The power law equation is fitted to the stress strain data without ultrasonic irradiation using least square regression. The regression gives the strength coefficient $K = 6.87 \times 10^4$ and the strain hardening coefficient $n = 0.06$. With the hardening model ready, the softening model is investigated by expressing the stress reduction in terms of the ultrasonic energy input. The relation between

stress reduction and ultrasonic energy input is first observed by Blaha and Langenecker [12]. Later, several researchers investigated the relation and proposed different models [13, 21, 22]. Moreover, it is reported by Blaha and Langenecker that the stress reduction is observed to be “directly proportional” to ultrasonic energy input [12]. Therefore we start investigating the relation between stress reduction and energy input with linear regression.

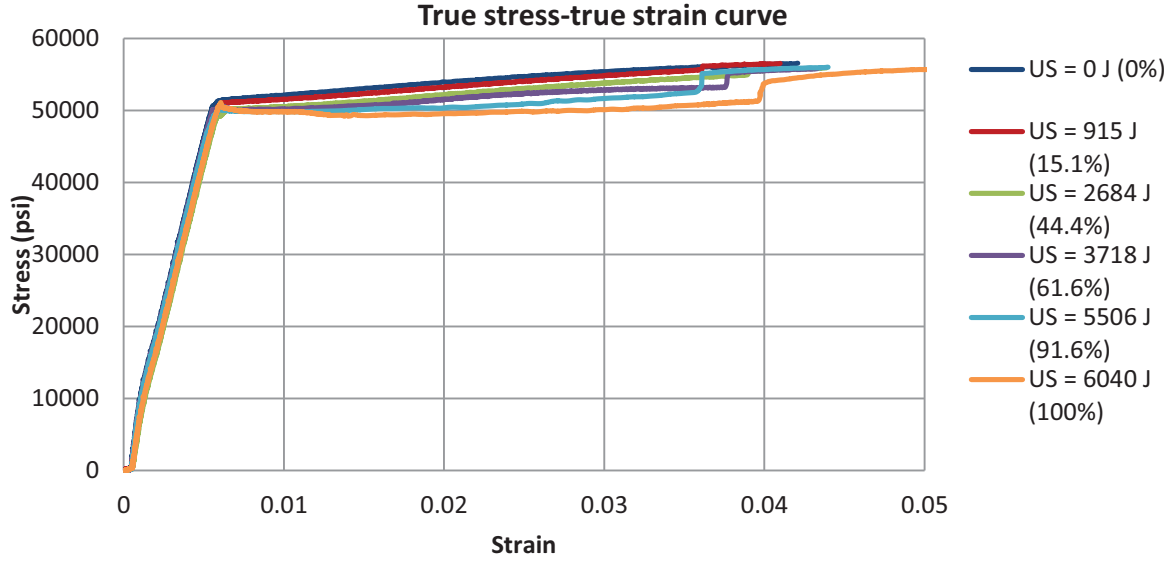


Fig.5 the true stress- true strain curves

Fig. 6 shows the relation between stress reduction and energy input. The horizontal axis represents the ultrasonic energy input E_u and the vertical axis represents the stress reduction ratio η . The stress reduction ratio is defined as:

$$\eta_i = \frac{\bar{\sigma}_0 - \bar{\Delta\sigma}_i}{\bar{\sigma}_0} \quad i = 1, 2, \dots, 6 \quad (5)$$

where $\bar{\sigma}_0$ is the averaged stress without ultrasonic irradiation, $\bar{\Delta\sigma}$ is the averaged stress reduction with ultrasonic irradiation. Since the instantaneous stresses are modeled with power law equations, the stress reductions are also in form of power law, i.e., the stress reduction varies as strain increases. However, within the strain range in test, the change of stress due to strain is much smaller than the stress reduction due to acoustic softening. As a result, the stress reductions are approximated as constant values which are calculated by averaging the stress reduction at true strain $\epsilon_{tr} = 0.02, 0.03$. The calculations are shown in Table 1. As ultrasonic energy increases, the softening curves tend to lose the hardening effect and transit to straight lines with slope. As a result, only curves with the five lowest ultrasonic energy levels are investigated. The other curve is modeled separately. A linear relation is established between energy input and the stress reduction ratio through linear regression:

$$\eta = 1 - dE_u \quad (6)$$

where $d = 1.21 \times 10^{-5}$. The coefficient of determination R^2 of the regression is 0.998, which shows that the experimental data fits well to the linear model. With both strain hardening model and acoustic softening model ready, the final analytical model is obtained by combining the two models:

$$\sigma_{soft} = \eta K \epsilon_t^n = (1 - dE_u) K \epsilon_t^n \quad (7)$$

where σ_{soft} represents the instantaneous true stress under ultrasonic irradiation. The curves with the first five levels of ultrasonic energy are characterized by the analytical model shown above. The curve with highest ultrasonic energy input, however, has to be modeled separately due to the observation that the hardening effect vanishes as the stress strain curve tends to become a straight line. Without changing the softening term η , the strain hardening model of the power law is replaced by a linear hardening model:

$$\sigma_t = a\varepsilon_t + b \quad (8)$$

where a and b are constants determined by curve fitting. The model for the last group of data with highest energy input yields:

$$\sigma_{soft} = \eta(a\varepsilon_t + b) = (1 - dE_u)(a\varepsilon_t + b) \quad (9)$$

By fitting the data to the replaced model, the coefficients are determined: $a = 5.55 \times 10^4$, $b = 5.25 \times 10^4$.

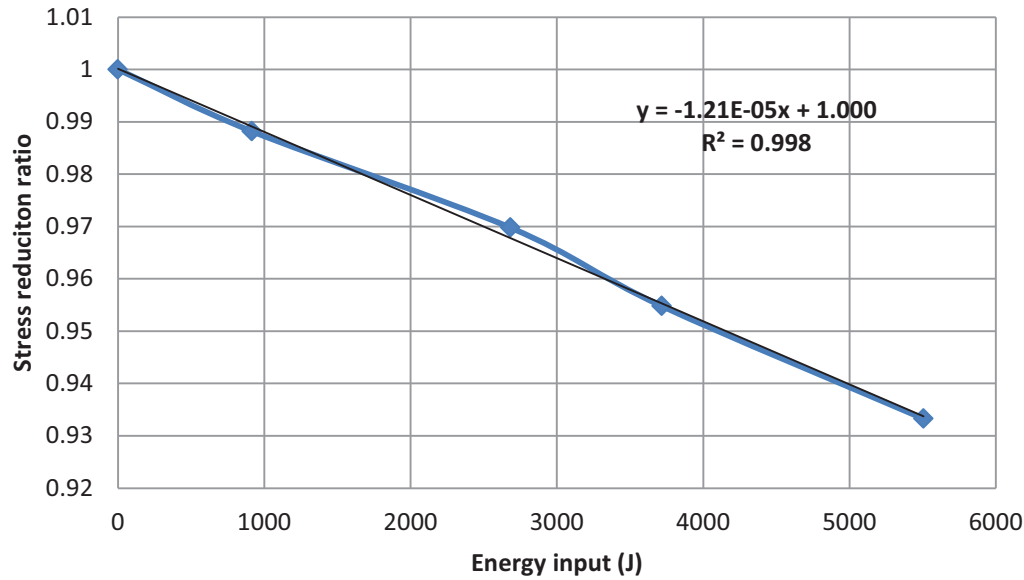


Fig. 6 The stress reduction versus ultrasonic energy input relation

Table 1. The calculation of stress reduction

Energy level (J) (E_u)	$\varepsilon_{tr} = 0.02$	$\varepsilon_{tr} = 0.03$	Average stress ($\bar{\sigma}$)	Averaged stress reduction ($\bar{\Delta\sigma}$)	Stress reduction Ratio (η)
0	53968	55387	54678	0	1.00
916	53222	54840	54031	646	0.99
2684	52163	53885	53024	1654	0.97
3718	51608	52801	52205	2473	0.96
5560	50378	51679	51028	3649	0.94
6040	49567	50118	49842	4835	0.92

Fig.7 shows comparisons of experimental data and numerical values predicted by the analytical model. The true stress strain curves are truncated and only the part of curves with

acoustic softening are displayed. The solid lines represent experimental data and the lines with markers represent the approximation made by the analytical models. It can be observed that the prediction from the analytic models agrees well with experimental data in the four lowest energy levels. In the fifth energy level, $E_u=5560$ J, the strain hardening is not significant at the beginning and the curve levels off. As deformation proceeds, the power-law shape strain hardening appears and the curve starts to agree with the prediction from the analytical model. In the last and the highest energy level, however, the acoustic softening is so significant that the power-law shape of the strain hardening is transformed into the linear shape of hardening. As a result, a linear hardening model has to be introduced instead for characterization. A good agreement is shown between the linear model prediction and the experimental data.

In summary, an analytical material model of aluminum 6061 is proposed to account for both acoustic softening and strain hardening that occur simultaneously as material deforms in plastic region. The ultrasound-induced stress reduction is proportional to ultrasonic energy input. The strain hardening behavior of the material, however, differs depending on the values of ultrasonic energy. With ultrasonic energy below a certain threshold, in this case 60% of the maximum energy input, the strain hardening displays a curved shape and can be modeled using power law equations. With ultrasonic energy above the threshold of 60%, however, the strain hardening diminishes and has to be modeled using a linear hardening model.

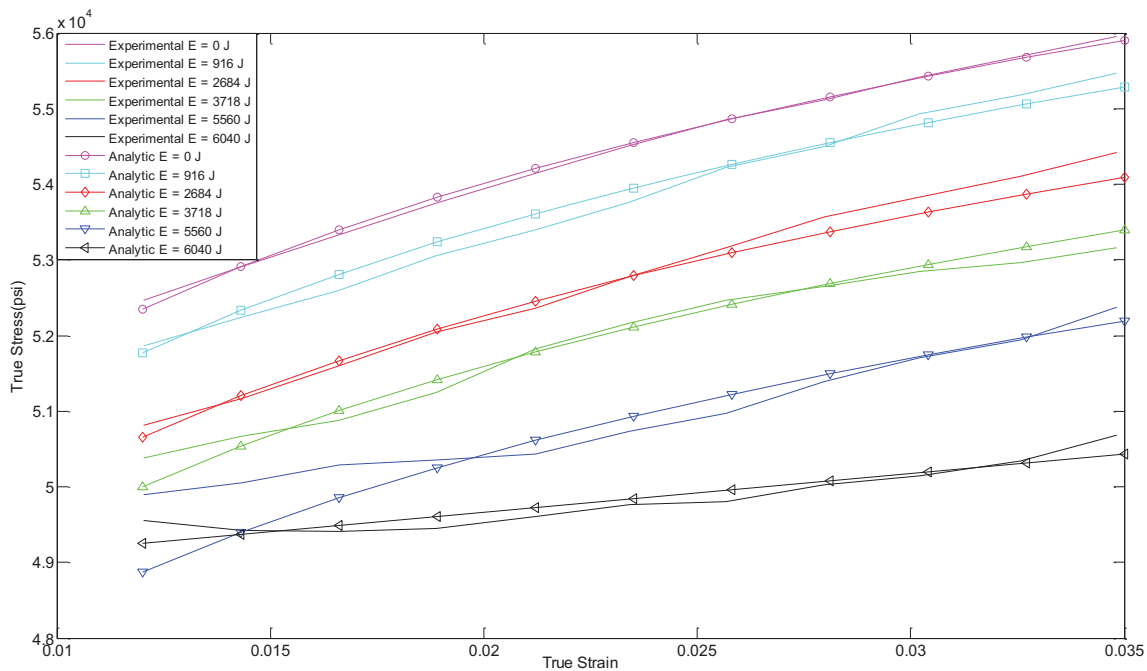


Fig. 7 The comparison of experimental data and prediction by analytical model

5. Discussion

In this paper, a series of experiments are conducted to characterize the acoustic softening of aluminum 6061 under different levels of ultrasonic energy input. However, some advantages and limitations of the experimentation need to be pointed out. First, the experimentation setup used in this paper proves to be more effective in reducing noise from thermal softening than

other designs [23]. The experimental setups for studies of acoustic softening vary in the literature. However, the method to observe acoustic softening is based on the stress strain diagram of materials. As a result, tensile or compression tests are conducted to achieve stress strain relations while transversal or longitudinal ultrasonic waves are applied to show the significance of ultrasound. Blaha and Langenecker, and some researchers [12, 27, 31] performed tensile tests on specimens while applying longitudinal ultrasonic waves. Culp and other researchers [21, 31-33] replaced tensile tests with compression tests while applying longitudinal ultrasonic waves. Siu et al. and Yao et al. [22, 34] proposed setups that apply ultrasonic wave in transversal directions during compression tests. Dutta et al. applied longitudinal ultrasonic waves in a direction perpendicular to the axis of the specimen during tensile tests. By evaluating these experimental setups, it is found that compression tests introduce more friction than tensile tests, and that transversal ultrasonic vibrations introduce more friction than longitudinal vibrations. As a result, the combination of tensile tests and application of longitudinal vibration reduces the noise from thermal softening by avoiding unnecessary frictions. Second, the ultrasonic energy levels used in the analytical model are measured from the electric power consumption which does not indicate the exact amount of energy that softens the specimen. It is extremely difficult to quantify the exact amount of energy input into specimen due to the difficulties in quantifying the energy losses during ultrasound propagation in the ultrasonic stack (transducer, booster and horn), specimens and frames. However, the objective of the analytical model is to characterize acoustic softening by means of investigating the relation between the stress reductions and the energy absorptions. By replacing the ultrasonic energy input with electric energy consumption, it is justifiable to assume that the relation between stress reduction and energy input remain unchanged. Therefore the electric energy input serves only as an indicator of ultrasonic energy input for the purpose of characterizing acoustic softening. Third, the geometry of the tensile specimens in use are different from that of ASTM standard specimens due to manufacturing limitations. Two fillets are designed for the specimen to transit large installation diameter to small testing diameter.

According to experimental observations, the stress is reduced by as much as 10%, which is not as significant as the reductions reported in the literature. Blaha and Langenecker observed stress reduction as high as 100% in aluminum single crystals [12]. Culp obtained approximately 50% stress reduction in aluminum 6063, 30% stress reduction in steel 1018 and less than 10% in magnesium [21]. Daud achieved approximately 25% stress reduction in aluminum 1050 [31]. Yao obtained roughly 50% stress reduction in aluminum 1100 [22]. In comparison, the aluminum 6061 has much higher yield strength than the materials in which large stress reductions are achieved and thus requires more energy input to achieve similar stress reduction. However, since the ultrasonic energy input is not available in many of the studies, the quantitative comparison becomes difficult.

6. Conclusion and Future Work

By designing the experimental setup that superimposes longitudinal ultrasonic wave to tensile test, the stress reduction of aluminum 6061 is measured at different levels of ultrasonic energy input. It is observed that:

- 1) The acoustic softening in aluminum 6061 is small compared with those in aluminum single crystals whereas the applied ultrasonic energy is much higher than that applied to aluminum single crystals.
- 2) A residual effect of softening is observed as soon as the ultrasound stops. The effect then diminishes as material deformation continues.
- 3) The stress reduction is observed to be linearly proportional to the ultrasonic energy input.

Based on the observation, an analytical model is established to characterize the acoustic softening effect. The power law model is able to capture the strain hardening as ultrasonic energy input is below a certain threshold; a linear hardening model is introduced to capture the strain hardening when ultrasonic energy input is high. The stress reduction is modeled by using a “softening term” which is proportional to ultrasonic energy input.

With the acoustic softening experimentally observed and analytically characterized, the future work includes observing and characterizing thermal softening effects, and establishing a UAM model in which both acoustic softening and thermal softening are implemented.

7. Acknowledgement

This research was partially supported by the National Science Foundation under grant # 1068977 entitled “Understanding the Macroscopic Dynamics of Ultrasonic Consolidation”. The views presented in this work do not necessarily reflect those of our sponsor whose support is gratefully acknowledged. We also wish to thank Ms. Sophie Morneau from Branson Ultrasonics Corporation for loaning some ultrasonic component.

References

- [1] Kong, C., Soar, R., & Dickens, P. (2003). Characterisation of aluminium alloy 6061 for the ultrasonic consolidation process. *Materials Science and Engineering: A*, 363(1), 99-106.
- [2] Ram, G. J., Robinson, C., Yang, Y., & Stucker, B. (2007). Use of ultrasonic consolidation for fabrication of multi-material structures. *Rapid Prototyping Journal*, 13(4), 226-235.
- [3] Zhang, C. S., & Li, L. (2009). A coupled thermal-mechanical analysis of ultrasonic bonding mechanism. *Metallurgical and Materials Transactions B*, 40(2), 196-207.
- [4] Cheng, X., & Li, X. (2007). Investigation of heat generation in ultrasonic metal welding using micro sensor arrays. *Journal of Micromechanics and Microengineering*, 17(2), 273.
- [5] De Vries, E. (2004). Mechanics and mechanisms of ultrasonic metal welding
- [6] Lee, S. S., Kim, T. H., Hu, S. J., Cai, W. W., Abell, J. A., & Li, J. (2013). Characterization of joint quality in ultrasonic welding of battery tabs. *Journal of Manufacturing Science and Engineering*, 135(2), 021004.
- [7] Joshi, K. C. (1971). The formation of ultrasonic bonds between metals. *Welding Journal*, 50(12), 840-848.
- [8] Cheng, X., & Li, X. (2007). Investigation of heat generation in ultrasonic metal welding using micro sensor arrays. *Journal of Micromechanics and Microengineering*, 17(2), 273.
- [9] Li, J., Han, L., & Zhong, J. (2008). Short circuit diffusion of ultrasonic bonding interfaces in microelectronic packaging. *Surface and Interface Analysis*, 40(5), 953-957.

- [10] Gunduz, I. E., Ando, T., Shattuck, E., Wong, P. Y., & Doumanidis, C. C. (2005). Enhanced diffusion and phase transformations during ultrasonic welding of zinc and aluminum. *Scripta Materialia*, 52(9), 939-943.
- [11] Kenik, E., & Jahn, R. (2003). Microstructure of ultrasonic welded aluminum by orientation imaging microscopy. *Microscopy and Microanalysis*, 9(S02), 720-721.
- [12] Langenecker, B. (1963). Effect of sonic and ultrasonic radiation on safety factors of rockets and missiles. *AIAA Journal*, 1(1), 80-83.
- [13] Siddiq, A., & El Sayed, T. (2011). Acoustic softening in metals during ultrasonic assisted deformation via CP-FEM. *Materials Letters*, 65(2), 356-359.
- [14] Kelly, G. S., Advani, S. G., Gillespie Jr, J. W., & Bogetti, T. A. (2013). A model to characterize acoustic softening during ultrasonic consolidation. *Journal of Materials Processing Technology*, 213(11), 1835-1845.
- [15] Blaha, F., & Langenecker, B. (1955). Tensile deformation of zinc crystal under ultrasonic vibration. *Naturwissenschaften*, 42(556), 0.
- [16] Langenecker, B. (1966). Effects of ultrasound on deformation characteristics of metals. *Sonics and Ultrasonics*, IEEE Transactions on, 13(1), 1-8.
- [17] Nevill, G., & Brotzen, F. R. (1957). The effect of vibrations on the static yield strength of a low-carbon steel. *Proceeding-American Society for Testing Material*, 57, 751-758.
- [18] Winsper, C., & Sansome, D. (1971). Application of ultrasonic vibrations to the plug drawing of tube. *Metal Forming*, 38(3), 71-75.
- [19] Biddell, D., & Sansome, D. (1974). The development of oscillatory metal-drawing equipment—an engineer's view. *Ultrasonics*, 12(5), 195-205.
- [20] Pohlman, R., & Lehfeldt, E. (1966). Influence of ultrasonic vibration on metallic friction. *Ultrasonics*, 4(4), 178-185.
- [21] Culp, D., & Gencsoy, H. (1973). Metal deformation with ultrasound. Paper presented at the 1973 Ultrasonics Symposium, pp. 195-198.
- [22] Yao, Z., Kim, G., Wang, Z., Faidley, L., Zou, Q., Mei, D., et al. (2012). Acoustic softening and residual hardening in aluminum: Modeling and experiments. *International Journal of Plasticity*, 39, 75-87.
- [23] Mao, Q., Gibert, J. M., & Fadel, G. (2014). Investigating the ultrasound-induced acoustic softening in aluminum 6061. *Proceedings of the ASME 2014 International Design Engineering Technical Conferences & Computers and Information in Engineering Conference (IDETC/CIE 2014)*, Buffalo, NY.
- [24] Hockett, J., 1967. On relating the flow stress of aluminum to strain, strain rate, and temperature. *Transactions of the Metallurgical Society of AIME* 239, 969–976.
- [25] Siddiq, A., & Ghassemieh, E. (2008). Thermomechanical analyses of ultrasonic welding process using thermal and acoustic softening effects. *Mechanics of Materials*, 40(12), 982-1000.
- [26] Lemaitre, J. (1994). *Mechanics of solid materials* Cambridge university press.
- [27] Mignogna, R., Green, R., Duke, J., Henneke, E., & Reifsnider, K. (1981). Thermographic investigation of high-power ultrasonic heating in materials. *Ultrasonics*, 19(4), 159-163.
- [28] Siddiq, A., & Sayed, T. E. (2012). A thermomechanical crystal plasticity constitutive model for ultrasonic consolidation. *Computational Materials Science*, 51(1), 241-251.
- [29] Kocks, U. (1987). Constitutive behavior based on crystal plasticity. *Unified constitutive equations for creep and plasticity* (pp. 1-88) Springer.

- [30] Krausz, A. S., & Krausz, K. (1996). Unified constitutive laws of plastic deformation Elsevier.
- [31] Daud, Y., Lucas, M., & Huang, Z. (2007). Modelling the effects of superimposed ultrasonic vibrations on tension and compression tests of aluminium. *Journal of Materials Processing Technology*, 186(1), 179-190.
- [32] Hung, J., Tsai, Y., & Hung, C. (2007). Frictional effect of ultrasonic-vibration on upsetting. *Ultrasonics*, 46(3), 277-284.
- [33] Huang, H., Pequegnat, A., Chang, B. H., Mayer, M., Du, D., & Zhou, Y. (2009). Influence of superimposed ultrasound on deformability of cu. *Journal of Applied Physics*, 106(11), 113514-113514-6.
- [34] Siu, K., Ngan, A., & Jones, I. (2011). New insight on acoustoplasticity–Ultrasonic irradiation enhances subgrain formation during deformation. *International Journal of Plasticity*, 27(5), 788-800.